Tetralin Hydrogenation over Supported Nickel Catalysts

Ahmed K. AlAsseel[†]* and S. David Jackson**

Centre for Catalysis Research, School of Chemistry, University of Glasgow,

Glasgow G12 8QQ, UK

e-mail: David.jackson@glasgow.ac.uk

* Authors to whom correspondence may be addressed.

† Present address: Research & Development Centre, Saudi Aramco, Dhahran, Saudi Arabia

ABSTRACT

An investigation was carried out to study the feasibility of using 5% nickel/alumina catalysts synthesised with different methods and metal precursors for the hydrogenation of tetralin. The catalysts were characterized using AAS, TGA, XRD, XPS, hydrogen chemisorption, surface area and pore volume analysis. The catalysts were tested in a continuous-flow, fixed-bed, reactor using solvent free tetralin feed under 5 barg hydrogen, 210 °C, a WHSV of 5 h^{-1}, and 7.5 H_2:HC ratio (GHSV 4220 h^{-1}). These reaction conditions were much milder than the ones reported in the literature but showed considerably higher catalytic activity even with low metal loadings. The study indicated that the product's isomer ratio was governed by kinetics. Indeed a remarkable difference was observed in the selectivity for the catalysts synthesised with different metal precursors in relation to *cis*:*trans* decalin ratios, where catalysts derived from nickel carbonate showed higher selectivity to *cis*-decalin compared to catalysts prepared from nickel nitrate. It was speculated that dispersion and particle size played an important role in this variance as suggested by XPS and hydrogen chemisorption. It was also found that this change in selectivity was not related to conversion. Similarly, different deactivation patterns were observed over these catalysts.

KEYWORDS: Hydrogenation, Tetralin, Decalin, Naphthalene, Nickel/Alumina Catalysts

1. INTRODUCTION

Hydrogenation of polyaromatic compounds to enhance the efficiency of diesel and Jet fuels has received considerable attention recently to comply with global fuel specification and overcome future limitations. Typically, diesel fuel is produced from middle distillate fraction after desulphurisation and denitrogenation treatments. The resultant product usually contains relatively high percentage of aromatics, which often have a very low cetane number and consequently reduce the efficiency of the fuel. Diesel fuel is also produced from the fluid catalytic cracking (FCC) unit by-product namely light cycle oil (LCO) which falls in the range of diesel fuel. The characteristic properties of LCO show high content of sulphur, nitrogen, and polyaromatic compounds (mostly diaromatic compounds). Therefore, hydrogenating multi-ring aromatics will result in a better diesel fuel blend that has a higher cetane number [1-4]. Similarly, Jet fuel is also affected by aromatic content, which reduces thermal stability of the blend. It has been reported in the literature that hydrogenated multi-ring products play an important role in improving the thermal stability and also preventing thermal degradation and solid-forming tendency of long-chain alkanes in the fuel blend [5].

Naphthalene is the simplest diaromatic product that has been considered as a representative model for polyaromatic compounds. The hydrogenation of naphthalene has received great attention in the literature. However, less attention has been paid to its partially hydrogenated product tetralin (tetrahydronaphthalene), although it is considered as the simplest form of monoaromatic product [3]. Naphthalene hydrogenation is accomplished by nickel sulphide or nickel molybdenum catalysts under severe reaction conditions using a fixed-bed reactor at 20 to 60 barg and 400 °C [6]. In contrast, higher catalytic activity is required to fully saturate both

naphthalene and tetralin to produce decalin (decahydronaphthalene) (**Scheme 1**). It has been reported by Cooper and Donnis that the hydrogenation rate of the last ring of naphthalene is 20 to 40 times slower than hydrogenating the first ring [7]. It was suggested that the resonance stabilisation of the monoaromatic ring and the reversible reaction could be the reason behind the difference in the hydrogenation rate [8].

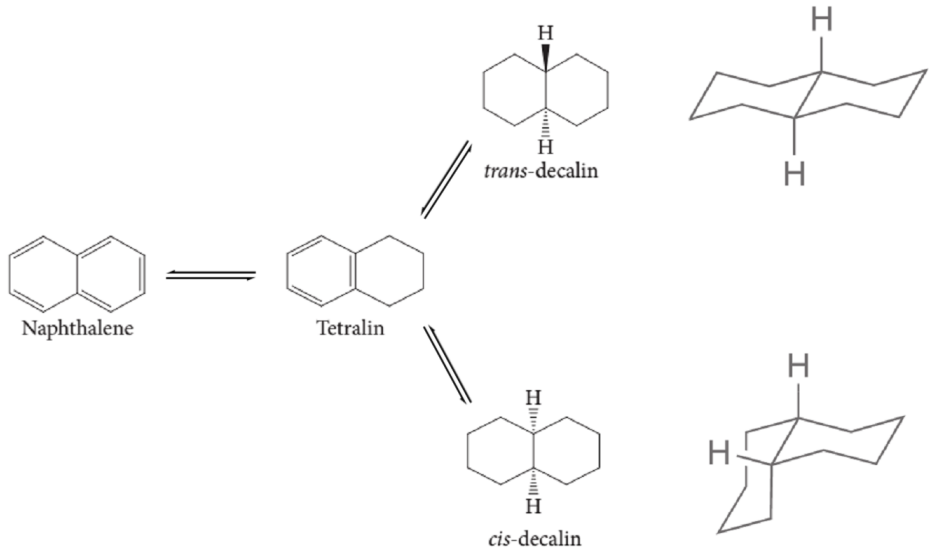

Scheme 1: hydrogenation of naphthalene and tetralin [3].

Conventionally, *cis*- and *trans*-decalin are produced by complete saturation of naphthalene, which incorporates tetralin as an intermediate reaction step. It is produced commercially with 97 wt.% purity [9-10]. The kinetic studies conducted in this regard by Sapre *et al.* and Huang *et al*. suggested first order reaction for both naphthalene and tetralin hydrogenation while Weitkamp suggested a zero order reaction for tetralin hydrogenation, which included octalins (octahydronaphthalenes) in their reaction scheme as an important intermediates [3,11-13]. Weitkamp and Rautanen *et al*. proposed that decalin isomer formation is totally influenced by the

structure of the two octalin intermediates (Δ9,10-octalin and Δ1,9-octalin) (**Scheme 2**). This scheme suggested that naphthalene and tetralin hydrogenation go through dihydronaphthalene and hexahydronaphthalene intermediates before they achieve octalins. Δ9,10-octalin intermediate is formed directly from hexahydronaphthalene hydrogenation, while Δ1,9-octalin is either produced from hexahydronaphthalene hydrogenation or from irreversible isomerisation of Δ9,10-octalin. It was proposed that Δ1,9-octalin does not isomerise to Δ9,10-octalin due to the fact that the hydrogenation rate of Δ1,9-octalin is too high, which will produce decalins in the presence of hydrogen rather than isomerise to Δ9,10-octalin. The hydrogenation of Δ9,10-octalin will only produce *cis*-decalin since the double bond in this intermediate is located in the bridging position and the hydrogen atoms addition can only be added to one side. On the other hand, Δ1,9-octalin has lower chemical stability compared to Δ9,10-octalin and hence it has higher hydrogenation rate as mentioned earlier. It can produce both *cis*- and *trans*-decalin depending on the location of the hydrogen atom in position 10. When the addition of the hydrogen atoms to positions 1 and 9 occur on the same side as the hydrogen atom in position 10; *cis*-decalin is produced. In contrast, *trans*-decalin is produced if the addition of the hydrogen atoms to position 1 and 9 occur on the opposite side of the hydrogen atom in position 10. It was assumed that these pathways go through stepwise of adsorption, desorption, and re-adsorption or direct hydrogenation of the intermediates [3].

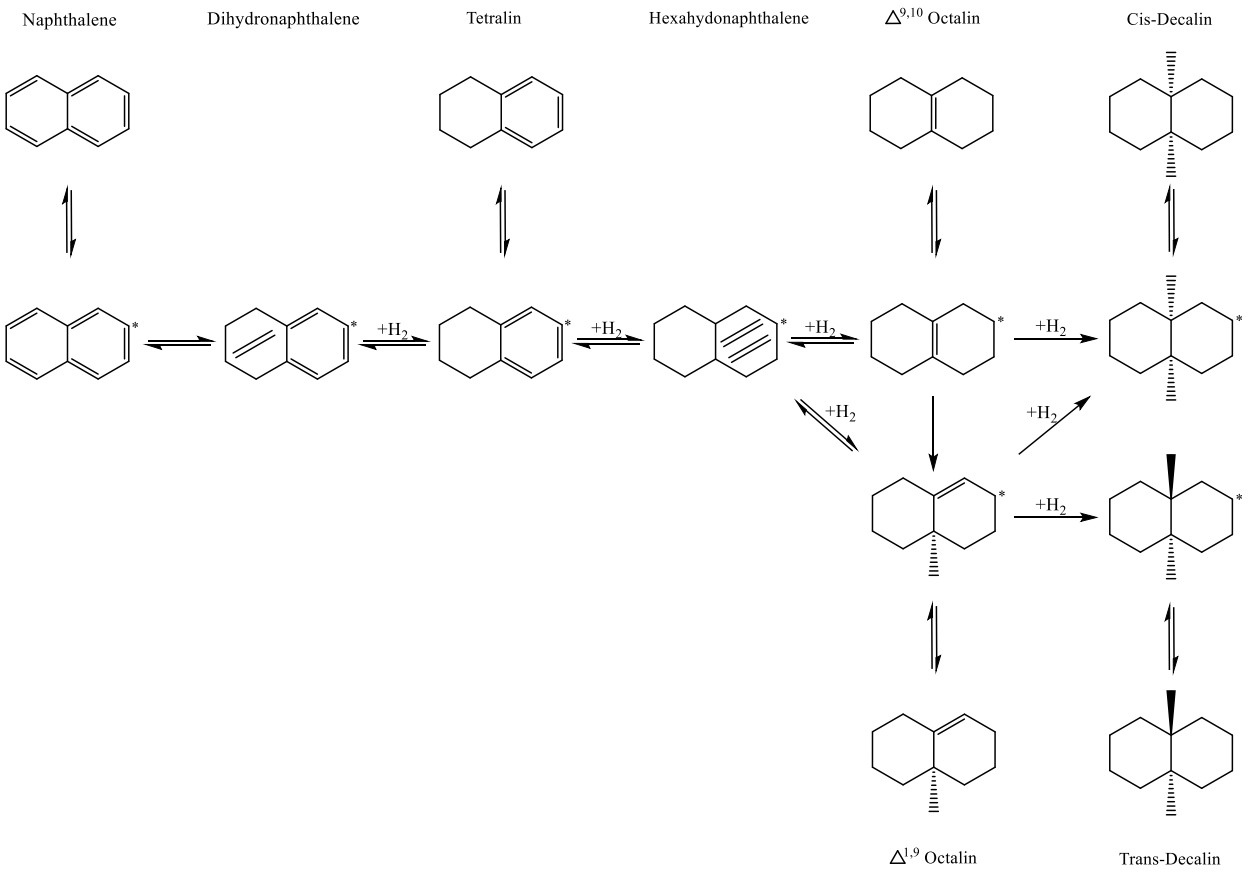

Scheme 2: Reaction scheme for tetralin hydrogenation. Surface adsorbed species are labelled with an asterisk. Reproduced with permission from ref. 3. Copyright (2001) Elsevier.

Based on the aforementioned aspects, the enhancement of this process has increased substantially in the recent years where several catalysts have been developed to boost the catalytic activity and selectivity of naphthalene and tetralin hydrogenation at moderate reaction conditions. Several studies have been conducted with the aim of studying the effects of altering the catalyst preparation methods and materials (*e.g*. supports and active metal) on the hydrogenation reaction, while other studies focused on investigating the influence of operating conditions and the effect of feed poisoning on the catalytic integrity and stability [1,4,5,12]. It was inferred from these studies that the hydrogenation reaction was greatly influenced by varying the preparation techniques and

the starting materials of the catalysts. This suggested that the change in the physicochemical properties of the catalysts can improve the catalyst activity and reliability. Similarly, the outcome of the reaction condition investigation showed prominent effects on the conversion and selectivity of this process.

Most of the studied catalysts for this process were supported noble metal catalysts [1, 5, 12]. These catalysts have remarkable characteristic properties that can hydrogenate naphthalene and tetralin at moderate temperature (*i.e*. 200 °C) and high hydrogen pressure but unfortunately they are not a desirable choice for this process owing to their cost and their vulnerability to sulphur compounds [5,14]. On the other hand, nickel catalyst has almost been neglected, although it has been reported as a good alternative to noble metals catalysts for aromatic compound hydrogenation [14]. In this regard, this project entailed synthesising nickel catalysts using several techniques and different metal precursors in order to produce catalysts with different properties and compare their effects on tetralin hydrogenation and decalin selectivity.

2. EXPERIMENTAL

2.1 Catalyst Synthesis.

2.1.1 Wet Impregnation:

Conventional wet impregnation (IMP) method [15-16] was employed since it is the most widely adopted technique to synthesise metal-supported catalysts. Several catalysts were synthesised using this method by loading as-received, trilobe θ-alumina pellets (≈1.5-5mm) (SGS Destpack) with different percentages of Ni from a nickel nitrate hexahydrate (Alfa Aesar) solution. The

calculated quantity of the metal precursor (0.57 g) was dissolved in minimal amount of demineralised water that was required to cover the support. Then, the metal solution was added to the calculated amount of alumina (2.19 g) by means of spraying the aqueous solution over the support. After that, the mixture was stirred and then left at room temperature for thirty minutes in order to settle and capillary action to take place. The obtained mixture was dried overnight at 80 °C and finally cooled to room temperature.

2.1.2 Precipitation-Deposition Impregnation (PD):

This technique was used to prepare two 5% Ni/Al_2O_3 catalysts using different metal precursors, denoted as (PD1 and PD2). The active metal was introduced by means of controlled precipitation of nickel on alumina using different metal precursors. In terms of the catalysts prepared, nickel nitrate precursor (0.57 g) was dissolved in 5 ml demineralised water and added in portions over an hour to the trilobe θ-alumina pellets (2.19 g) that were suspended in another 5 ml portion of demineralised water while heating at 90 °C. The suspension was stirred and acidity maintained at pH 6 by adding few drops of nitric acid. In the case of nickel carbonate, the insoluble precursor (0.25 g) was mixed with the trilobe θ-alumina pellets (2.19 g) in 10 ml demineralised water. Then, nitric acid was added dropwise over one hour while stirring and heating at 90 °C. The addition of nitric acid slowly converted insoluble metal carbonate into soluble nitrate form which controlled the release of the metal in the solution. Finally, the resultant mixture was transferred to an oven and kept at 80 °C to dry overnight. Similar procedures were described elsewhere [16-17].

2.1.3 Ammonia Evaporation Method:

Similarly, two supported 5% Ni catalysts were synthesised by the ammonia evaporation technique using different metal precursors and denoted as (HDC1 and HDC2) [18-21]. The following procedures were performed according to Gelder [21]. The catalysts in this technique were prepared in two stages. The first stage was the preparation of metal ammonia complex. The calculated amount of ammonia solution (2.8 ml, 25 %, Sigma Aldrich) and demineralised water (5 ml) were added to a round-bottomed flask and mixed thoroughly. Then, ammonium carbonate chips (0.2 g, ACS reagent, Sigma Aldrich) were added and the mixture agitated by a mechanical stirrer (200 rpm) until all the chips were dissolved completely. Finally, the nickel precursor (0.57 g for nickel nitrate or 0.25 g of nickel carbonate) was added to the solution in portions with constant stirring over a period of time and heated at 90 °C (the solution colour changed from green to blue). The final catalyst was obtained in the second stage where metal ammine solution was added to a 10 ml round-bottomed flask fitted with a reflux condenser in a rotary evaporator and the pH of the solution was monitored. Subsequently, the trilobe θ-alumina pellets (2.19 g) were added slowly to the stirred solution (260 rpm). The solution was heated to 90 °C and refluxed to distil off the ammonia. After 30 minutes, it was observed that the colour of the support had changed from white to green in a colourless solution and the pH of the reaction mixture stabilised. The stabilisation of the pH and the colour change indicated that all the ammonia was removed and the deposition was completed. After 10 minutes, the solution was transferred to a beaker and dried overnight at 80 °C.

2.2 Catalyst Characterization.

2.2.1 Surface Area and Pore Volume Analysis:

This analysis was performed to determine the surface areas and total pore volumes of the fresh and spent catalysts. It was executed using a Micromeritics Gemini Analyser. A standard preparation procedure was followed to analyse the samples. Samples were ground to a fine powder using a mortar and pestle before 0.05 g of the sample was placed in the sample tube and heated to 110 °C, under flowing nitrogen gas for 16 h to remove moisture and any contaminants. Finally, the sample was analysed using Micromeritics Gemini Analyser and the collected measurements were used to determine the surface area and total pore volume of the sample.

2.2.2 Atomic Absorption Spectroscopy (AAS):

Elemental analysis was carried out using a Perkin Elmer Analyst 400 to determine the actual percentage of metal in the synthesised catalysts. The analysis entailed preparing series of reference standards to calibrate the instrument in addition to sample preparation. The sample was prepared by dissolving approximately 0.1 g of the catalyst sample in *aqua regia* solution. This was followed by several dilutions of the sample solution to bring them to a linear range with the reference standards. Then, the measurement was conducted in the analyser using nickel hollow cathode lamp. The measured absorption was applied in the calibration curve to determine the unknown concentration of the metal.

2.2.3 X-Ray Powder Diffraction Analysis:

X-ray powder diffraction (XRD) was utilized to determine the catalyst crystalline inorganic phases/compounds in the fresh catalysts. In this analysis, a PANalytical X'Pert XRD equipped with copper tube was used following the standard procedure. A calcined (at 500 °C) supported metal catalyst was ground to a fine powder using a mortar and pestle. The fine powder sample was

mounted on the XRD sample holder to acquire the diffraction patterns from 5° to 85° with a step size of 0.02°. The identification of the inorganic crystalline compounds present in the catalyst samples was achieved using PANalytical X-Pert High Score Plus software combined with the International Centre for Diffraction Data (ICDD) and powder diffraction file (PDF) database of the standard reference materials.

2.2.4 Thermogravimetric Analysis:

An SDT Q600 Thermogravimetric analyser (TGA) coupled with a mass spectrometer (MS) was used to provide information on the removal of material from fresh and spent catalysts in addition to the activation of the fresh calcined catalyst samples as a function of increasing temperature. The samples were analysed using this instrument to perform temperature programmed oxidation (TPO) analysis from ambient temperature to 1000 °C at a rate of 10 °C per minute under 2% O_2/Argon. The fresh catalyst samples were analysed to determine the catalyst thermal stability and the temperature required for calcination to remove nitrate and carbonate from the fresh catalyst. TPO was also carried out on the spent catalyst samples to determine the amount and the nature of carbon laydown on the catalyst. Additionally, temperature programmed reduction (TPR) was carried out on calcined catalyst samples from ambient temperature to 1000 °C at a rate of 10 °C per minute under 5% H_2/N_2 atmosphere in order to determine the reduction temperature of the catalyst by means of introducing hydrogen to remove oxygen in order to activate nickel.

2.2.5 X-ray photoelectron spectroscopy:

The X-ray photoelectron spectroscopy (XPS) analysis was carried out at the Drochaid Research Services (St Andrews) using KRATOS Axis Ultra DLD instrument. This technique was utilised

to measure the composition on the surface of the catalyst and to determine the oxidation state of the metal. The samples were prepared by mounting 20 mg of calcined catalyst (at 773K) on a molybdenum sample holder and then analysed by the XPS. The analyser was operated at fixed pass energy of 160 eV for the survey spectrum and 40 eV for the individual regions. The measurements were carried out using monochromatic Al Kα X-rays source. Due to the nature of the material, neutralisation was necessary during the acquisition to reduce the charging effects on the analysed samples.

2.2.5 Hydrogen Chemisorption:

This measurement was performed using Micromeritics ASAP 2020 Surface area and porosity analyser at the Drochaid Research Services (St Andrews). The purpose of this analysis was to measure the hydrogen uptake to calculate metal dispersion, metal particle diameter, and metal surface area. In each run, approximately 250 mg of the calcined ground catalyst was loaded in the sample tube. Prior to the measurement and after loading the sample, the tube was purged with helium for 30 min at 100 °C and then evacuated at 450 °C for 5 min. Subsequently, the catalyst was reduced *in-situ* at 450 °C for 4.5 hours with a ramp rate of 10 °C per minute. After reduction, the system was evacuated at the same temperature to remove any residual hydrogen. Finally, the sample was cooled down to room temperature and hydrogen uptake was measured.

2.3 Catalyst Evaluation.

Catalytic activities of the synthesised catalysts were determined using a ½ inch, continuous down-flow, glass-lined, fixed-bed reactor. Prior to the reaction, the catalyst was calcined at 500 °C for 30 min. Then, approximately 2.3 g of the catalyst was loaded as pellets into the tube and

backed with glass beads beds above and beneath the catalyst bed. Subsequently, the catalyst was reduced *in-situ* in a flow of hydrogen (60 $ml.min^{-1}$) at atmospheric pressure at 450 °C for 4.5 h. A solvent free feed (tetralin 98+%, Acros Organic) was supplied by means of HPLC pump (11.8 $ml.h^{-1}$) where it was mixed with hydrogen and carried through the catalyst bed. The organic components of the reactor effluent were condensed for sampling while the rest of the eluant was vented. The catalytic activity was measured at different temperatures (180-280 °C), pressures (5-15 barg), and hydrogen flow rates (60-340 $ml.min^{-1}$) for 30 h. All reactions were carried out at fixed space velocities (i.e. WHSV=5 h^{-1} and LHSV= 3 h^{-1}) while the H_2/tetralin molar ratio varied for these reactions. The condensed product was collected every hour and analysed using Trace GC ultra 2000 series. The GC was equipped with a flame ionization detector and 150 m Petrocol DH capillary column. At the end of the reaction, the HPLC pump was turned off and the reactor was left for 30 min under hydrogen flow to flush the catalyst bed and then the spent catalyst was collected and sealed in a glass vial for further analysis.

3. RESULTS AND DISCUSSION

3.1 Catalyst Characterization.

3.1.1 Physical and Textural Properties Characterization:

The preliminary physical and textural characterization results of the synthesised catalysts are summarized in **Table 1**. The obtained characteristic properties revealed that the synthesised catalysts were significantly influenced by the preparation techniques. The catalyst properties were also impacted by changing the metal precursor for each technique. The measurements of metal loading using atomic absorption spectroscopy indicated that the highest loadings were achieved

by impregnation and HDC techniques using nickel nitrate and nickel carbonate. On the other hand, the lowest metal loading was measured for both precipitation-deposition (PD) catalysts produced using both precursors. In terms of surface area and total pore volume, the results indicated that impregnation technique decreased surface area and pore volume while PD and HDC techniques generally increased them, except for some individual catalysts like HDC1. The decrease in the surface area of the impregnated catalysts and the increase in the PD and HDC catalysts were in line with the literature [17, 21-22]. The pore distributions of the catalysts were all similar at ~15 nm, the same as the starting alumina. Catalysts PD2 and HDC2 showed slightly different behaviour in that as well as the pores at 15 nm, PD2 had new pores at 5 nm, while HDC2 showed pores at 10 nm.

Table 1: Physical and textural characterization data of the synthesised calcined catalyst.

Sample	Sample description	Measured metal loading (wt.%)	Surface area (m^2/g)	Total pore volume (cm^3/g)
Alumina	Unloaded sample	0	98	0.46
IMP1	5% Nickel nitrate on alumina (impregnation)	4.8	92	0.41
PD1	5% Nickel nitrate on alumina (precipitation-deposition)	3.1	100	0.48
HDC1	5% Nickel nitrate on alumina (HDC)	4.3	89	0.41
PD2	5% Nickel carbonate on alumina (precipitation-deposition)	3.2	112	0.47
HDC2	5% Nickel carbonate on alumina (HDC)	4.2	121	0.49

3.1.2 Thermal Properties Characterization:

Temperature programmed oxidation (TPO) and reduction (TPR) were carried out using the TGA-MS with oxidising (2 % O_2/Ar) and reducing gas 5 % H_2/N_2) respectively on the five catalysts in addition to the alumina support and the nickel precursors as references. The TPO was used to specify the calcination temperature and the TPR, the reduction temperature. Different thermal profiles were obtained for each catalyst. **Figure 1** shows a weight loss between 25-200 °C that could be attributed to moisture adsorbed in the catalyst samples (confirmed by mass spectrometric analysis). Furthermore, different gases were released during TPO analysis from each catalyst depending on the metal precursor used during their synthesis. For instance, nitrogen monoxide evolution was evident from all catalyst samples that were prepared using nickel nitrate in addition to sample PD2, where the nitric acid was used during the synthesis. On the contrary, carbon oxides were evolved from samples synthesized using nickel carbonate. Based on the TPO analysis, the calcination temperature for all the catalyst samples was selected to be 500 °C. TPR profiles showed two distinct weight losses and a small shoulder (**Figure 2**) for all the catalysts. The first weight loss (~100 °C), in all samples, can be ascribed to removal of adsorbed moisture. The remaining weight loss and shoulder (> 400 °C) were assigned to the reduction of various nickel species in the samples. The TPR of the calcined nickel precursor (see Supplementary data **Figure S2**) showed only one event that started around 300°C, which was assigned to the reduction of bulk nickel oxide and involved hydrogen consumption and water production. Therefore, the second feature in the thermal profiles of the synthesised catalysts between 400-750 °C can be linked with reduction of nickel oxide specie. The reduction was shifted to a higher temperature in the synthesised catalyst due to the strong interaction between nickel oxide and the support. Finally,

the small shoulder around 800°C can be attributed to the reduction of nickel aluminate spinel. These results were in good agreement with the literature where reduction events at 400-750 °C and the shoulder around 800°C were assigned to reduction of nickel oxide and nickel aluminate respectively [23-25]. Based on the TPR analysis, the reduction temperature for all the catalyst samples was selected to be 450 °C to reduce nickel oxide species and minimize sintering effects.

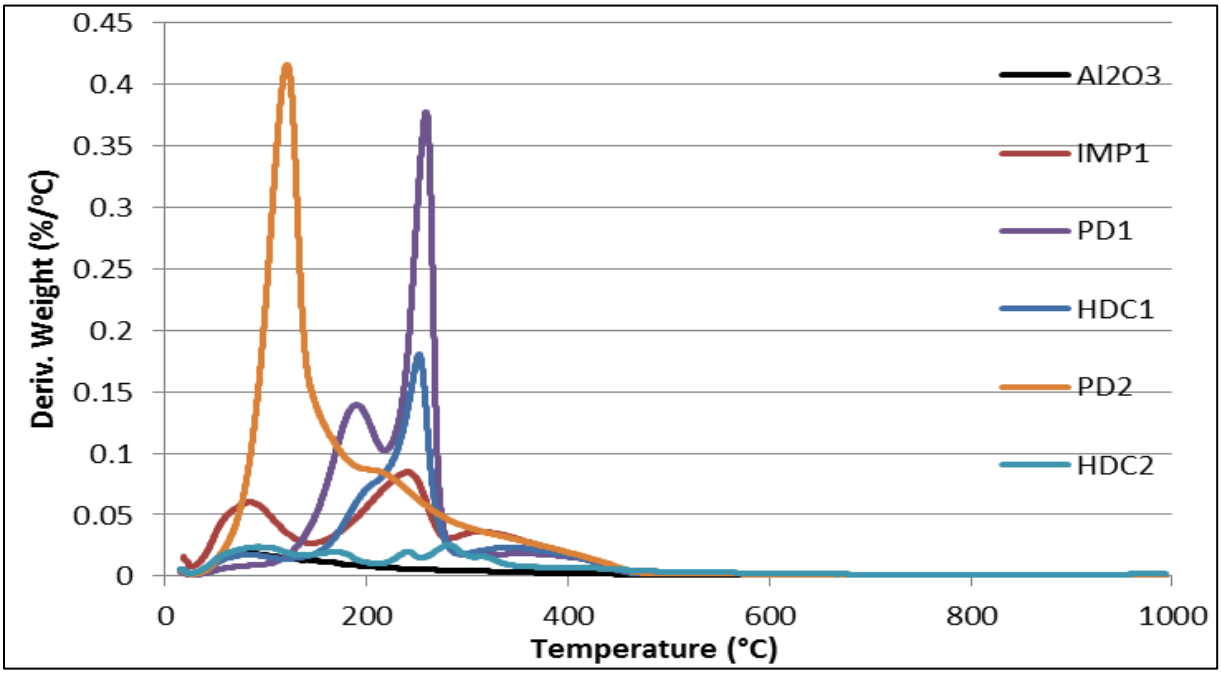

Figure 1: Temperature programmed oxidation for the synthesised catalysts showing the derivative of the weight loss.

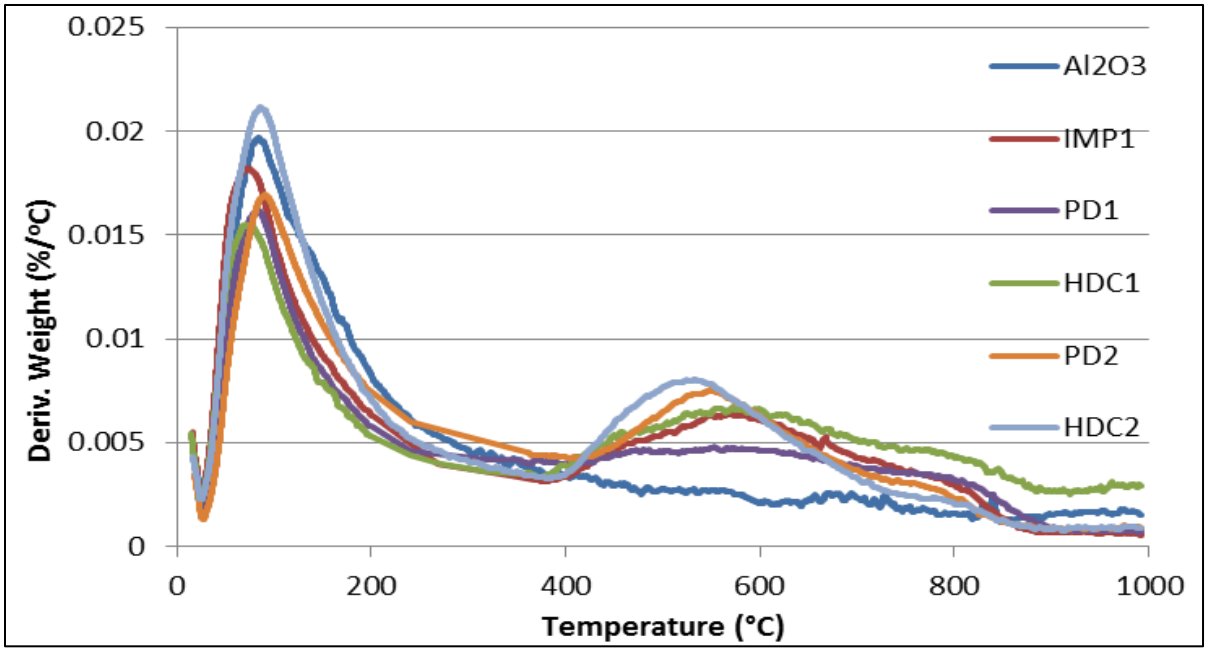

Figure 2: Temperature programmed reduction for the synthesised catalysts, showing the derivative of the weight loss curves.

3.1.3 Structural Characterization:

The XRD characteristic properties were studied for the synthesised catalysts in addition to the calcined alumina and calcined nickel precursors (nickel oxide) (**Figures 3 and 4**). The identification of the diffractograms for all the synthesised catalyst showed a good match with θ-alumina diffraction pattern. The low quantities of the loaded metal can result in higher dispersion with smaller particle sizes which in turn reduces the detectability of the nickel particles by the XRD. In addition, the overlap between alumina peaks and nickel peaks makes it much more difficult to identify Ni species in the obtained diffractograms of the synthesised catalysts. Chou and co-workers have reported in their study to characterize nanosized nickel particles that elemental nickel peak was positioned at 44.3° while NiO was positioned at 43.3° [26]. This agreed with the obtained diffractograms of the calcined nickel precursors (nickel oxide). However, no

sign of nickel reflections were observed in the synthesised in-house catalysts, which could be due to the aforementioned constraints.

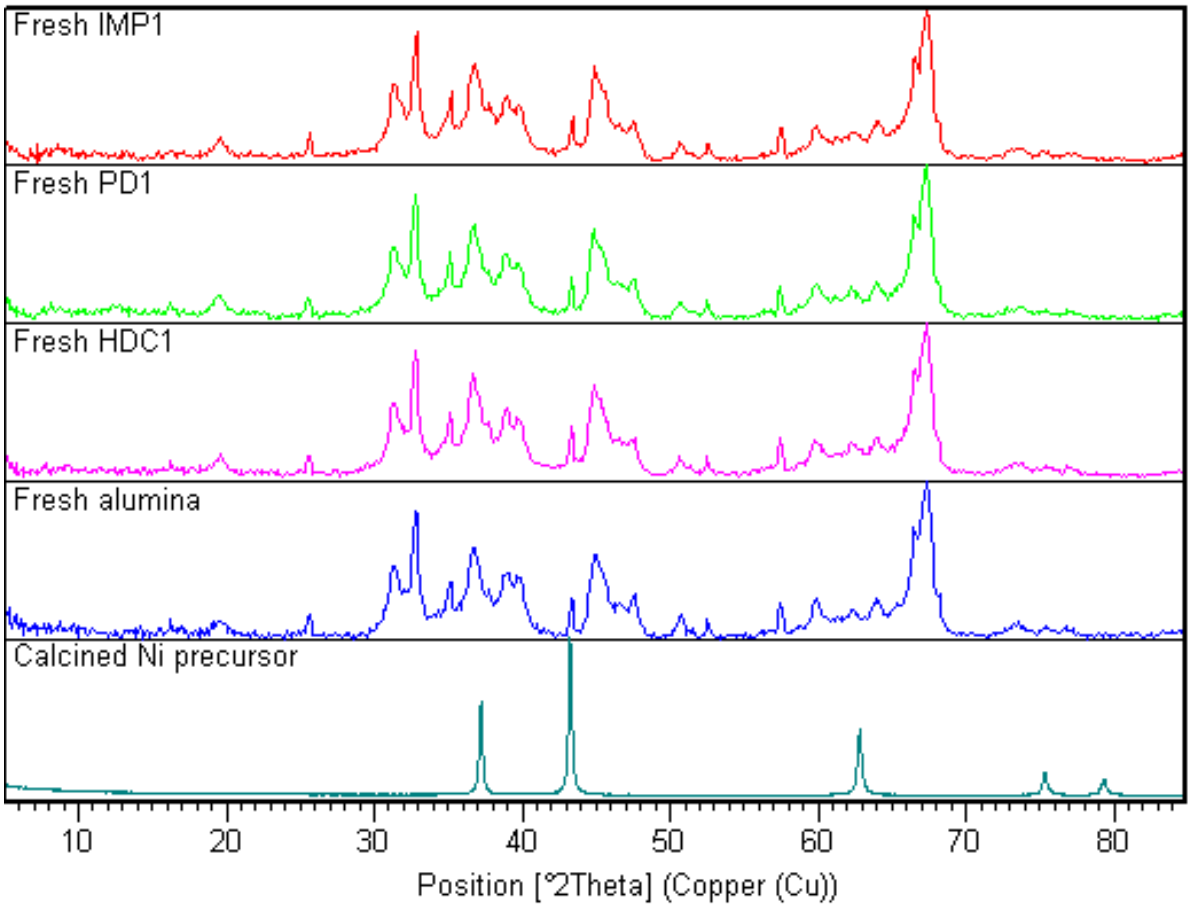

Figure 3: XRD diffractograms for the catalysts synthesised with nickel nitrate together with the alumina support and the calcined metal precursors (calcined nickel nitrate precursor gave identical XRD patterns identified as nickel oxide).

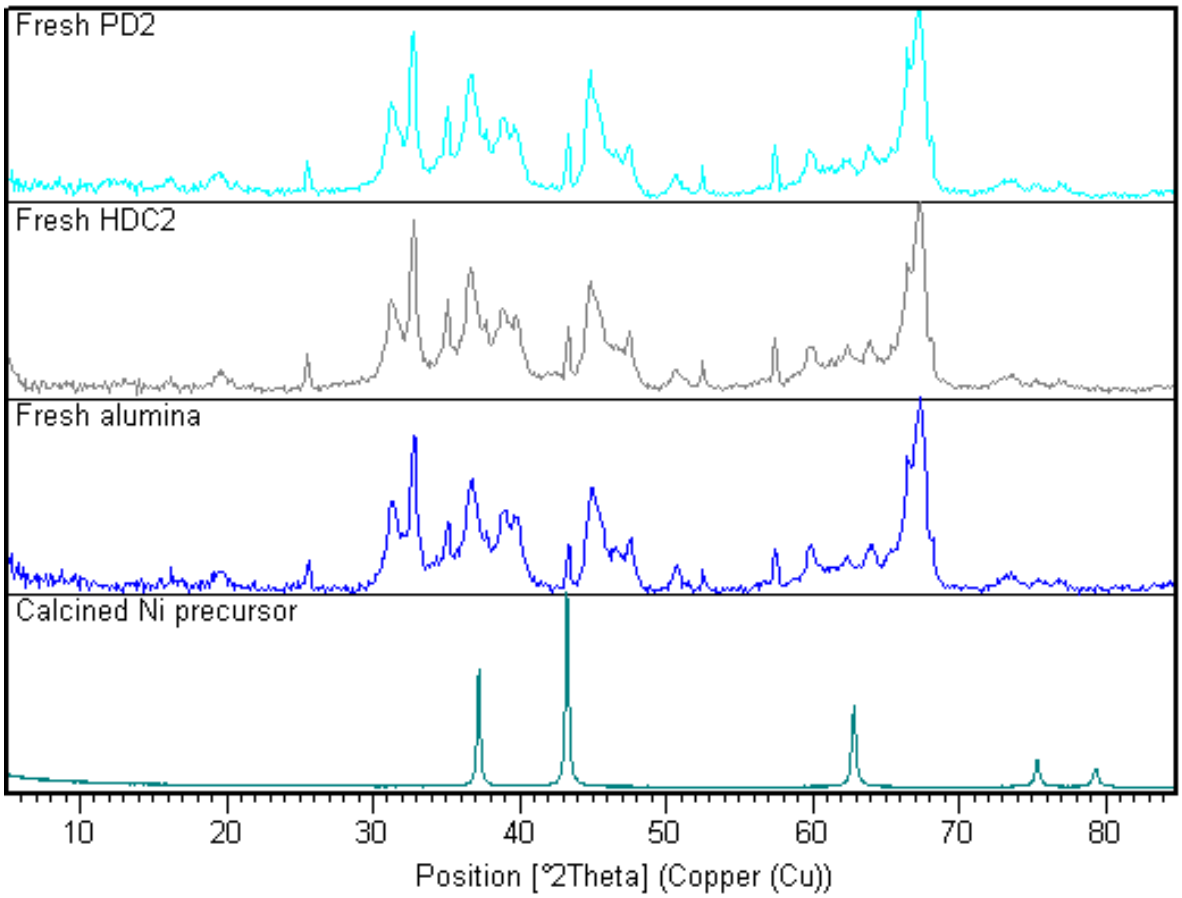

Figure 4: XRD diffractograms for the catalysts synthesised with nickel carbonate together with the alumina support and the calcined metal precursor (calcined nickel carbonate precursor gave identical XRD patterns identified as nickel oxide).

3.2 Catalyst Evaluation.

A catalytic activity test was performed on the unloaded alumina support. Negligible catalytic activity was measured for the alumina under conditions of 15 barg, 230 °C, and 60 ml.min^{-1} H_2 flow for 30 h continuous operation. The hydrogen/tetralin molar ratio for this reaction was 1.8. The effect of temperature was investigated over the HDC2 catalyst. The results are shown in

Figure 5. The catalyst was held at each temperature for 7 h and the data reported is that of the results after 7 h. These results show that above 230°C, dehydrogenation to naphthalene is readily observed and that optimum tetralin conversion was seen at around 210°C. Therefore, this temperature was chosen as the temperature at which the comparative tests would be undertaken. In general, the detected products in these reactions were mainly unreacted tetralin and decalin isomers with appreciable quantities of 1,9-octalin, 9,10-octalin, and naphthalene in some cases. Mass loss calculations gave a mass balance of 97±3% for all catalysts which is within the experimental limitations of the system.

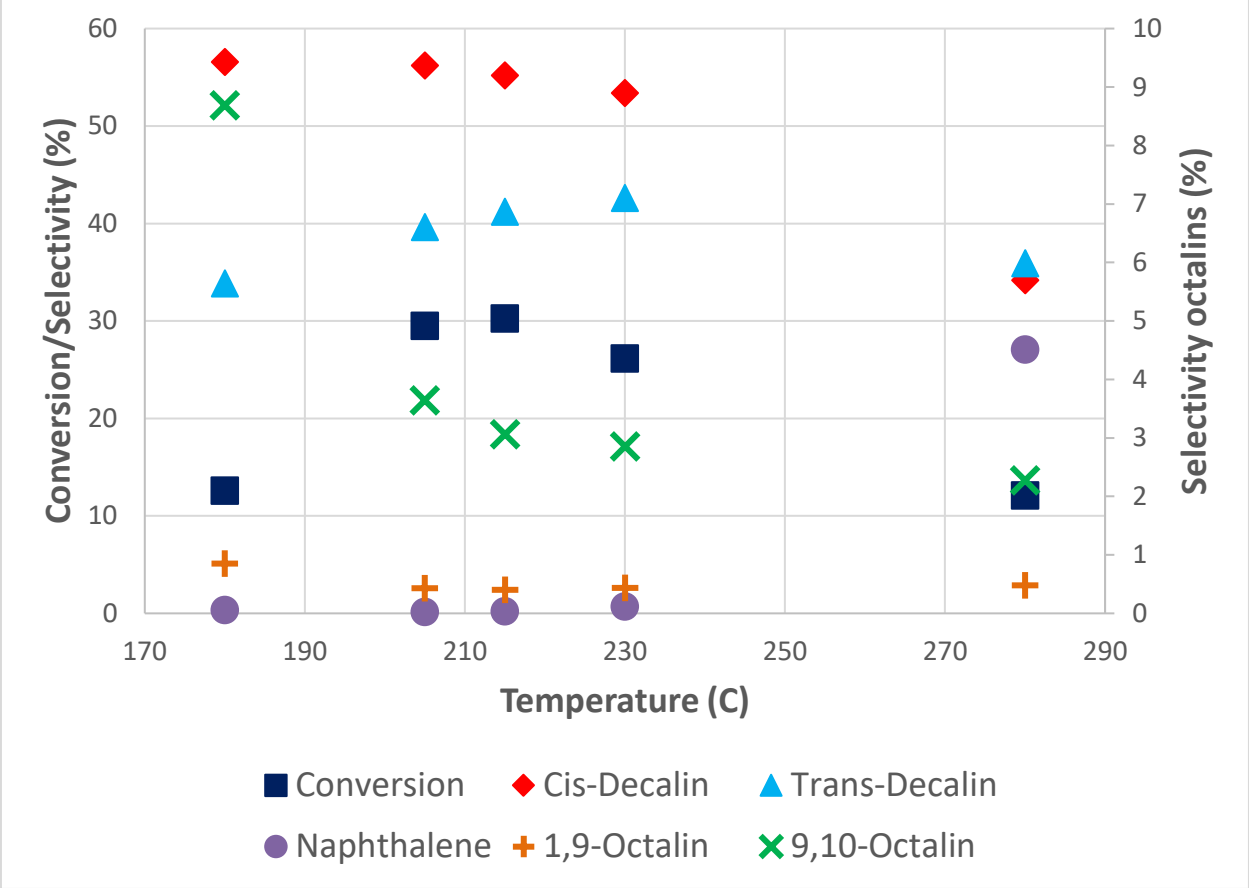

Figure 5. Testing of catalyst HDC2 at different temperatures. Conditions: 5 barg, 4.3 H_2:HC, the catalyst was held for 7 h at each temperature and the data relates to the end of the 7 h period.

3.2.1 Influence of Preparation Technique and Metal Precursor:

A set of operating conditions were selected (see Supplementary data section **S2**) to compare the synthesised catalysts (*i.e.* 5 barg, 210 °C, 7.5 H_2/HC ratio, and 4220 h^{-1} GHSV). Each catalyst was tested twice (fresh batch for each run) to explore reproducibility of the results (see Supplementary data section **S3**). The results revealed that the highest conversion was achieved by the catalyst synthesized with impregnation technique using nickel nitrate followed by the catalysts synthesised with HDC technique using both nickel nitrate and nickel carbonate (**Figure 6**). The initial activity

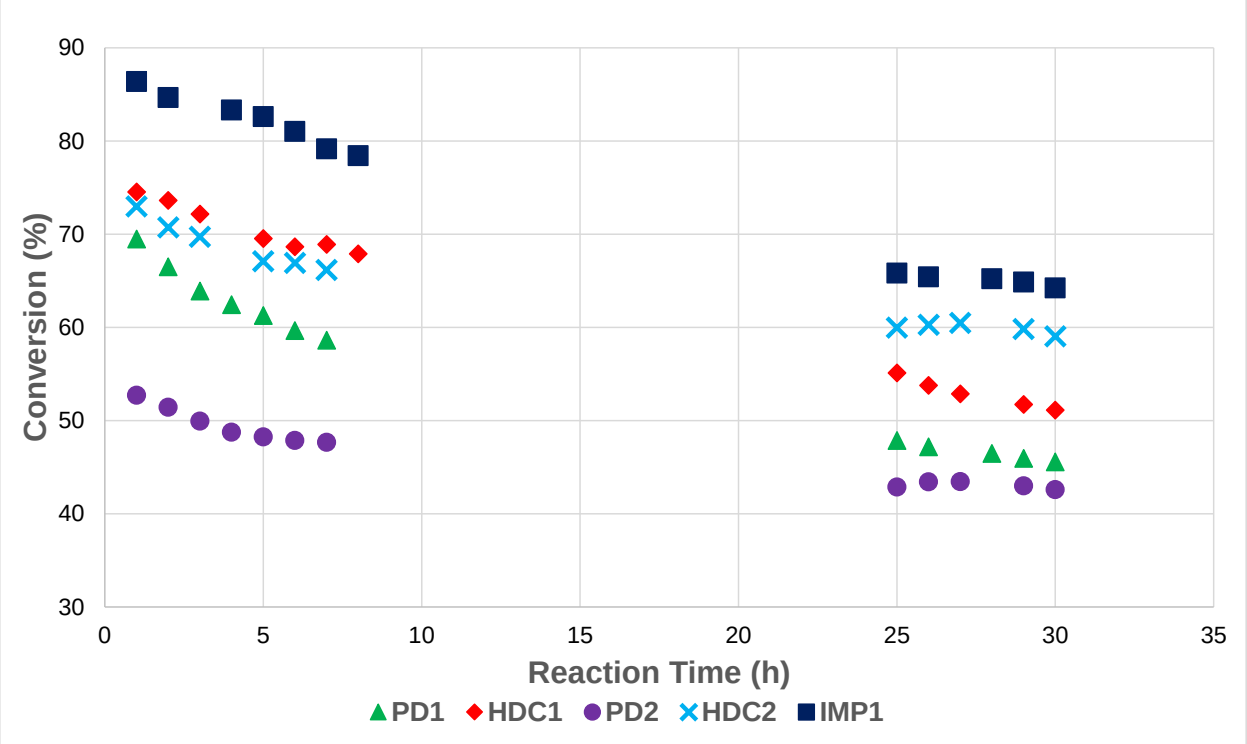

Figure 6: Tetralin conversion for all the catalysts under 5 barg, 210 °C, and 240 $ml.min^{-1}$ of H_2 flow (7.5 H_2/HC ratio) for 30 h time-on-stream.

sequence of the catalysts followed the metal loading percentage measured by AAS, where the highest activity was measured for the highest metal loading (*i.e.* the impregnated catalyst) except PD1 catalyst which exhibited higher activity than its weight loading would suggest (**Figure 7**). Note that the HDC2 catalyst showed much higher activity than that observed during the temperature study since it was evaluated at higher H_2/HC ratio,

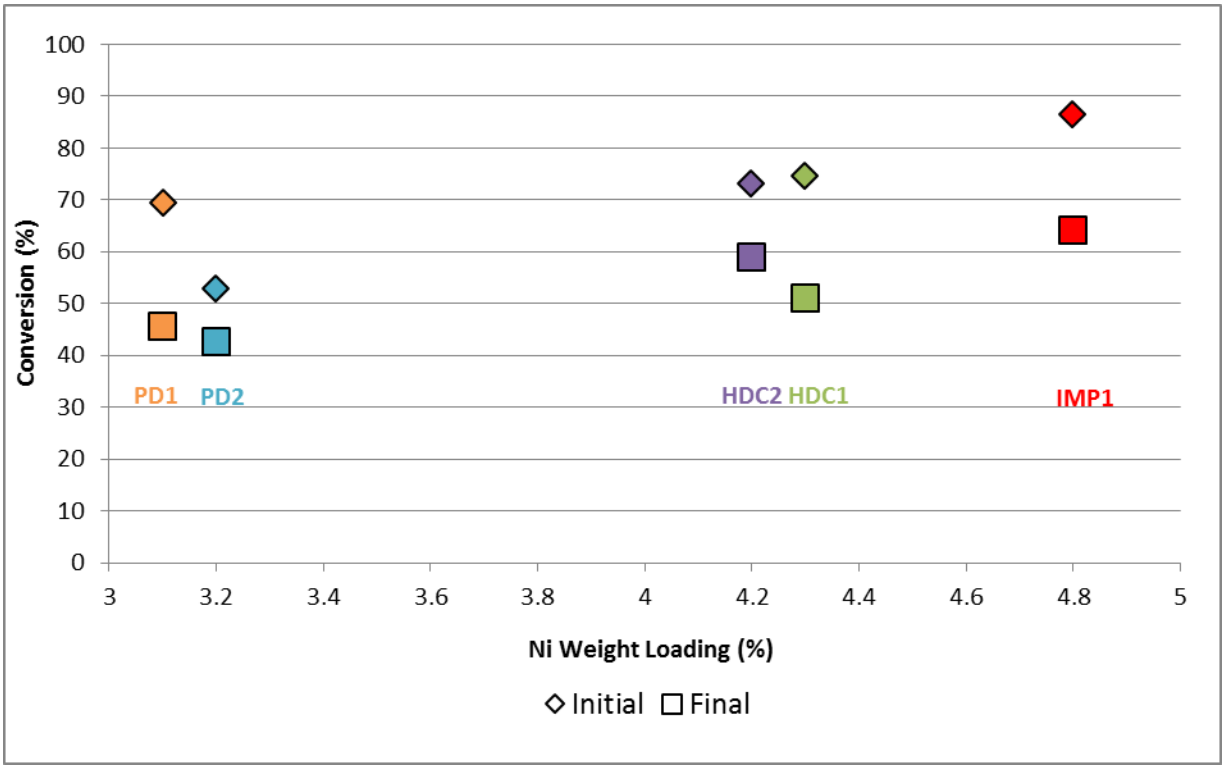

Figure 7. Initial and final (30 h) conversion as a function of metal loading.

To confirm that conversion was proportional to the percentage of the loaded metal, a series of catalysts were synthesised with nickel nitrate using impregnation technique to prepare 2.5, 5, and 7.5% nickel loaded systems (**Table 2**). The results indicated that the activity is directly proportional to the metal loading (**Figure 8**). The *trans* to *cis* ratio for both the 7.5 and 5% catalysts were similar while the 2.5% catalyst gave a slightly lower ratio. The ratio of

$\Delta^{9,10}$-octalin:$\Delta^{1,9}$-octalin intermediates also increased with catalyst loading. The equilibrium ratio of $\Delta^{9,10}$-octalin:$\Delta^{1,9}$-octalin at 210 °C is ~3.5 [13], however the ratio observed was always greater and as the loading was increased the ratio moved further away from equilibrium as expected if the $\Delta^{1,9}$-octalin reacted faster than the $\Delta^{9,10}$-octalin.

Table 2: Physical and textural characterization data of the fresh and spent catalysts synthesised with different loadings.

Sample	Fresh Catalysts			Spent Catalysts		
	Measured metal loading (wt.%)	Surface area ($m^2.g^{-1}$)	Total pore volume ($cm^3.g^{-1}$)	Surface area ($m^2.g^{-1}$)	Total pore volume ($cm^3.g^{-1}$)	TPO Weight loss (wt.%)
IMP2.5	2.5	85	0.39	83	0.47	1.28
IMP5	4.8	92	0.41	81	0.43	1.10
IMP7.5	7.6	80	0.47	75	0.39	0.56

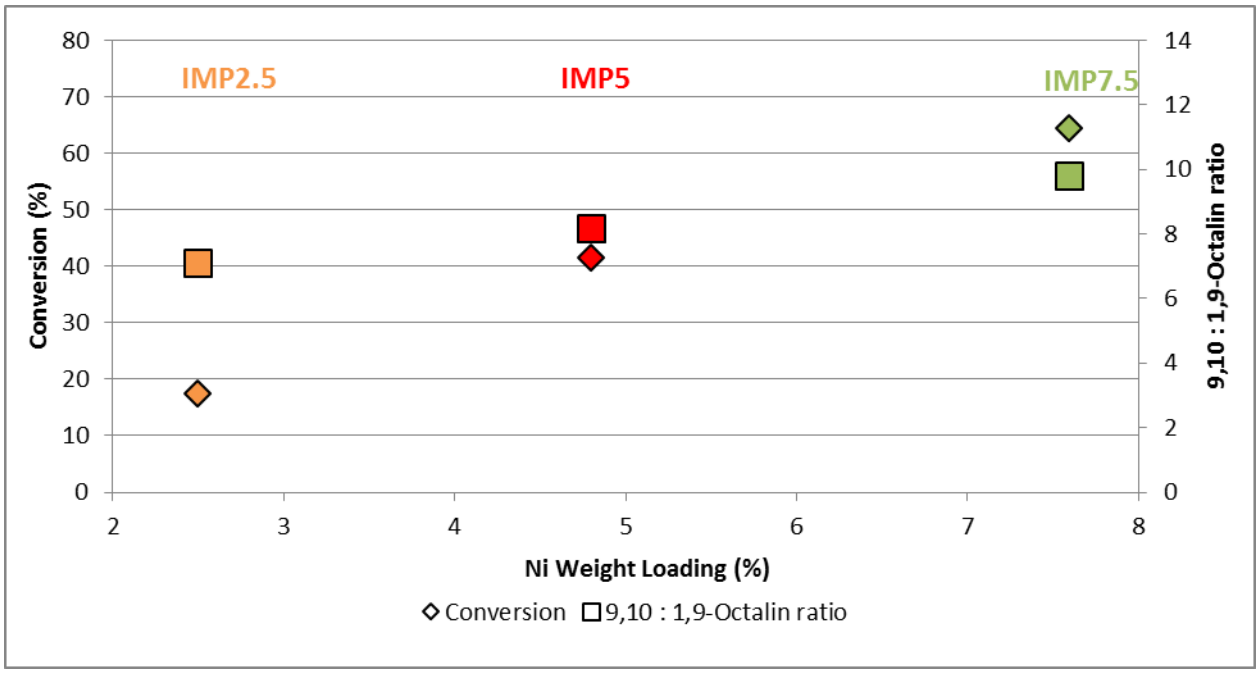

Figure 8: Activity test results for the catalysts prepared with different loading under 5 barg, 210 °C, and 140 ml.min^{-1} of H_2 flow (4.3 H_2/HC ratio) after 7 hours.

Figure 6 also reveals that the rate of deactivation is affected by the choice of metal precursor rather than the method of catalyst preparation in that the deactivation rate for catalysts synthesised with nickel nitrate is higher than the ones synthesised with nickel carbonate. The nitrate derived catalysts typically lost ~23 % conversion over the length of the test (30 h), whereas the carbonate derived catalysts lost only ~10 %. Another notable difference between the catalysts synthesised with different metal precursors is the selectivity, where nitrate derived catalysts were selective to *trans*-decalin while the nickel carbonate catalysts were more selective to *cis*-decalin (**Figure 9**). Therefore, altering preparation technique using the same metal precursor showed variations in conversion but the *trans*/*cis*-decalin ratio almost remained constant, indicating that activity and selectivity were controlled by different factors. The thermodynamic equilibrium ratio calculation for *cis* and *trans*-decalin indicates that *trans*-decalin is favoured at lower temperatures, with it

making up approximately 95.5-94.5 % of total decalins at 210 °C [3, 27]. Clearly, the isomer ratio obtained from the carbonate-derived catalysts is governed by kinetic rather than thermodynamic constraints.

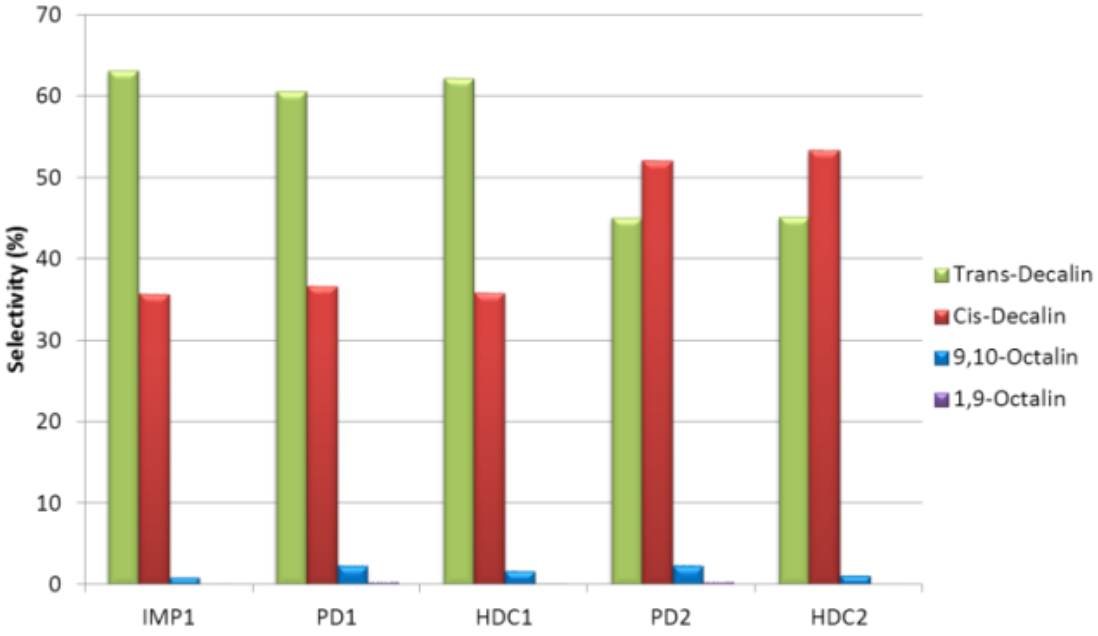

Figure 9: Reaction selectivity for all the catalysts under 5 barg, 210 °C, and 4220 h^{-1} GHSV (7.5 H_2/HC ratio) for 30 h.

Jongpatiwut *et al*. suggested that *cis-trans* isomerisation may take place in these reactions and could affect the observed *trans* to *cis* ratio in the hydrogenation reaction [28]. Similarly, Dokjampa *et al*. stated that the selectivity solely depended on the catalyst used during the hydrogenation reaction as this affected the site competition between tetralin and decalin as well as the intrinsic rate of *cis* to *trans* isomerisation [15]. It was also mentioned that isomerisation was suppressed at low conversion due to the strong adsorption of tetralin while at high conversion, the concentration of *trans*-decalin increased because of *cis*-decalin isomerisation [15]. Nonetheless, most literature studies showed higher selectivity for *trans*-decalin using either precious metal catalysts or nickel

catalysts except the catalysts that utilized platinum as their active component [29-30]. To investigate this, an isomerisation reaction was carried out under the same conditions as above using a known mixture of decalin (60:40 *trans*:*cis* ratio) as a feed to test the isomerisation ability of both IMP1 and HDC2 catalysts. The results showed low activity for both catalysts where they achieved an average of 4-5% conversion for the isomerisation of *cis*-decalin to *trans*-decalin changing the ratio to (65:35-64:36) for both IMP1 and HDC2 catalysts. Therefore, the *cis* to *trans* ratio in the hydrogenation reactions was not significantly affected by decalin isomerisation. This is in agreement with other literature [3, 14]. To ensure that the differences in decalin selectivity were not related to changes in conversion, selectivity was compared at a common tetralin conversion for IMP1, HDC1, and HDC2 and the results are depicted in **Figure 10**. These results show a difference between IMP1 and HDC1(nitrate derived catalysts) in relation to HDC2 (carbonate derived catalyst) not only in the trans:cis-decalin ratio but also the selectivity to the octalin isomers. Both $\Delta^{9,10}$-octalin and $\Delta^{1,9}$-octalin can form *cis*-decalin but only $\Delta^{1,9}$-octalin can produce the *trans*-isomer after desorption and re-adsorption [8, 13]. HDC2 which gives a high *cis*-decalin yield has a low octalin yield suggesting a more rapid rate of octalin hydrogenation. Therefore, as the conversion from tetralin is the same, the decalin isomer selectivity is determined by the rate of hydrogenation of the octalin isomers.

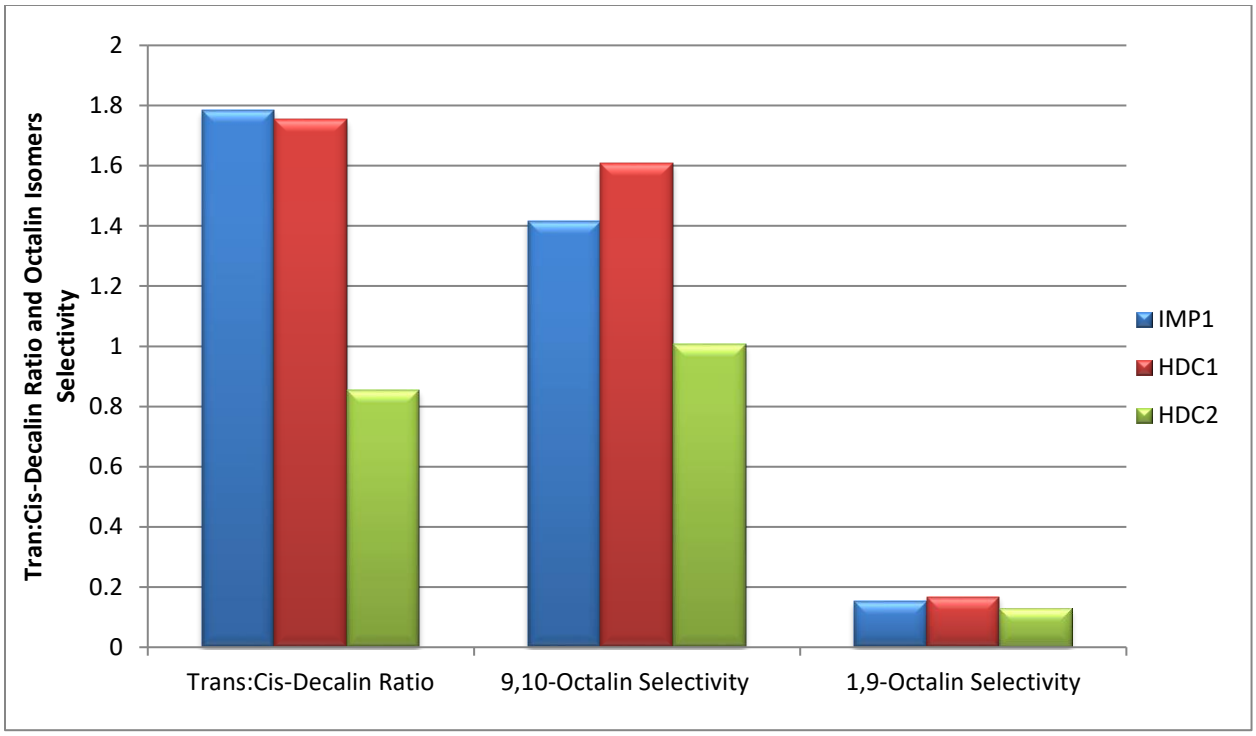

Figure 10. Comparison of octalin isomer selectivities and trans/cis-decalin ratio at ~64 % tetralin conversion for catalysts HDC1, HDC2 and IMP1. Conditions: 5 barg, 210 °C, GHSV 4220 (7.5 H_2/HC ratio).

Two catalysts (IMP1 and HDC2) were selected as representative samples for catalysts that exhibited different selectivity and were subjected to further characterisation. **Table 3** contains the hydrogen chemisorption and XPS analysis results for IMP1 and HDC2 catalysts. Hydrogen chemisorption revealed that the IMP1 catalyst had higher dispersion and metal surface area and hence a smaller particle diameter compared to HDC2. XPS analysis of the Ni 2p spectra confirmed only the presence of Ni^{2+} for both catalysts. However, the composition analysis obtained from the XPS indicated that the mass concentration of the nickel in the HDC2 catalyst was higher than the IMP1 catalyst. This revealed that the HDC technique dispersed most of the metal on the surface of the support and attenuated the alumina signal. This behaviour has been made use of for

determining dispersion in a series of HDC catalysts [20]. In contrast the impregnation technique dispersed the metal on the surface and inside the pores. Thus, higher dispersion and smaller particles were observed on the IMP1 catalyst while the reverse was measured for the HDC2 catalyst as the metal particles were agglomerated on the surface.

Table 3: Hydrogen chemisorption and XPS analysis results.

Sample	Hydrogen chemisorption				XPS Sample composition		
	H_2 uptake (cm^3/g)	Ni dispersion (%)	Mean particle diameter (nm)	Ni surface area (m^2/g)	[Ni] mass %	[Al] mass %	[O] mass %
IMP1	0.924	5.1	20	1.6	8.9	42.3	48.8
HDC2	0.564	3.5	29	1.0	24.2	29.5	46.3

Therefore, from this analysis it would be expected that, as observed, catalyst IMP1 would be more active purely on the basis of nickel surface area. However, there is nothing to indicate why there is a change in selectivity. The system may be thought of as a classic A → B → C reaction, with A → B, tetralin to octalin aromatic hydrogenation and B → C, octalin to decalin olefin hydrogenation. The conversion data reveals that the precursor does not control tetralin hydrogenation (aromatic hydrogenation), therefore the control of selectivity comes in the conversion of the octalins (olefin hydrogenation). The XPS analysis indicated that residual carbonate or nitrate was not present and it is unlikely that the different preparation methods would give identical residual counter-ion amounts. Hence, we can propose that the selectivity of the systems is being controlled by the physical properties of the catalysts such as active metal location, metal particle size, and shape as defined by the metal precursor. Eliche-Quesada et al. [31]

synthesised several supported nickel zirconium-doped mesoporous silica catalysts using an impregnation technique and different metal precursors namely, aqueous nickel nitrate solution (Ni(Nit/A)), nickel nitrate ethanolic solution (Ni(Nit/E)), and aqueous nickel citrate solution (Ni(Cit/A)). The evaluation results of that study indicated that 2.6, 3.4, and 7.3 *trans* to *cis* ratio were achieved by Ni(Nit/E), Ni(Nit/A), and Ni(Cit/A) catalysts respectively. The study suggested that the variation in the selectivity was dependent on the nickel salt used in the catalyst preparation. However, the chemisorption characterisation results revealed that the average particle diameters were 41.5, 29.1, and 7.6 nm for Ni(Nit/E), Ni(Nit/A), and Ni(Cit/A) respectively. Thus, it can be inferred from this study that different metal precursor resulted in different dispersion and different particle size where *trans*-decalin was favoured when the catalyst had high dispersion and small particle diameter. This would also be in keeping with other studies of olefin hydrogenation where the shape and crystal face of the metal crystallite affect selectivity and *cis/trans* isomerisation [32-33]. Our results also agree, with the IMP1 catalyst having smaller particle size and higher *trans:cis* ratio than the HDC2 catalyst. The difference in observed *trans:cis* ratio between studies relates to differences in reaction conditions.

3.3 Catalyst Post-Reaction Characterization.

There are several factors that can affect the deactivation rate of catalysts which includes reaction conditions as well as the physical and chemical characteristic properties of the catalysts. Since these catalysts were tested at the same reaction conditions, it was speculated that the difference in their properties was the driver that caused the variation in the deactivation rate. The characterisation results suggested that the common property between the catalyst prepared with nickel carbonate, which is different than the catalysts prepared with nickel nitrate was observed in

the surface area and pore volume analysis results, where PD2 and HDC2 exhibited smaller pore diameter as mentioned earlier. This would be in agreement with literature findings [34-36] where smaller pore sizes reduced the deactivation rate.

A set of physicochemical analyses were carried out on the spent catalysts that had been evaluated at 5 barg, 210 °C, and GHSV 4220 h^{-1} (7.5 H_2/HC ratio) for 30 h. In the TPO analyses, the obtained thermal profiles showed two weight losses in all the spent catalyst samples (see Supplementary data section **S4**). The first weight loss was associated with desorption of moisture and removal of carbonaceous material, while subsequent weight loss was assigned to the combustion of other carbonaceous materials retained on the catalyst. The high percentage of coke on the unloaded alumina sample suggests that the coke formation occurred on the surface of the support rather than solely on the metal. The mass spectra for the evolved carbon dioxide (**Figure 11**) revealed several combustion events that can be related to different carbonaceous material deposited on the surface of the catalyst. Moreover, the average weight losses associated with the carbon combustion were in the range of 1.2-1.7 wt.% for all the spent catalysts except the unloaded alumina support (**Table 4**). These findings were supported by the BET analysis which revealed that the spent catalysts have lower surface areas compared to the fresh ones. This suggests that the catalyst deactivation was caused by coke formation. However, it can be seen in **Figure 11** that the carbon combustion event at ~150 °C is not present for both catalysts prepared by precipitation-deposition, while only the IMP1 catalyst does not have a combustion event at ~450 °C. Thus, there is not a simple link between carbon deposition and catalyst deactivation. Also, the differences in carbon deposition do not match with the changes in selectivity.

Typically, low temperature combustion is related to the combustion of molecular entities. The presence of molecular species on the used catalysts was confirmed by refluxing spent catalysts

with hexane and the solution analysed by GC revealing the presence of tetralin, decalins and naphthalene. Indeed, catalysts PD1 and PD2 do show a weight loss event at < 200 °C but no combustion, which may suggest that the preparation-deposition technique does not produce a nickel catalyst that is good at low temperature hydrocarbon combustion. Naphthalene combustion over metal oxides including nickel typically takes place below 200 °C [37- 38]. The main combustion event at ~350 °C can be associated with high H:C ratio fragments bonded to the surface and hydrogen was co-eluted with carbon dioxide, which is consistent with this interpretation. The higher temperature combustion of carbonaceous residues on the surface is likely to be associated with naphthalenic fragments, whereas the lower temperature event would relate to combustion of tetralin/decalin fragments.

Table 4: Physical and textural characterization data of the fresh and spent catalysts synthesised with different methods and metal precursor.

Sample	Fresh Catalysts			Spent Catalysts		
	Measured metal loading (wt.%)	Surface area ($m^2.g^{-1}$)	Total pore volume ($cm^3.g^{-1}$)	Surface area ($m^2.g^{-1}$)	Total pore volume ($cm^3.g^{-1}$)	TPO Weight loss (wt.%)
Alumina	0	98	0.46	88	0.47	5.80
IMP1	4.8	92	0.41	85	0.43	1.23
PD1	3.1	100	0.48	84	0.46	1.74
HDC1	4.3	89	0.41	85	0.39	1.43
PD2	3.2	112	0.47	95	0.39	1.71
HDC2	4.2	121	0.49	110	0.45	1.75

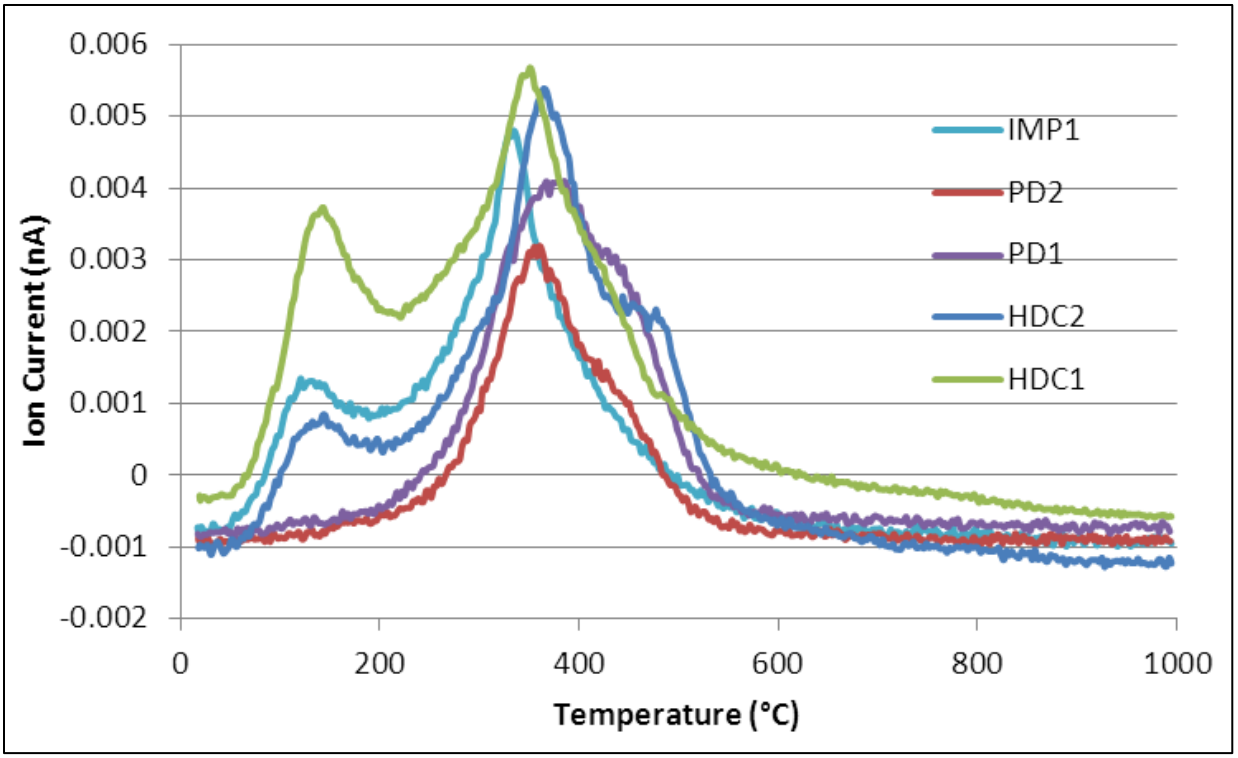

Figure 11: CO_2 evolution from the spent catalysts evaluated at 5 barg, 210 °C, and 240 ml.min^{-1} of H_2 flow (7.5 H_2/HC ratio) for 30 hours

3.4 Catalyst Benchmarking.

A comparison between the synthesised catalysts and the literature catalysts was carried out to benchmark the catalytic activity of the synthesised in-house catalysts. To the best of our knowledge, nickel catalysts have been investigated for tetralin hydrogenation in limited number of papers (less than 10), while most of the literature focused on precious metal catalysts to enhance the hydrogenation of fused ring aromatics. However, most of the papers reported very low activity for nickel catalysts. The highest nickel catalytic activities achieved in the literature for tetralin hydrogenation are tabulated in **Table 5**. The table shows that some of these catalysts were loaded with high percentage of nickel and evaluated as powder, which played a role in boosting their

catalytic activities. In terms of reaction conditions, they were tested at relatively high hydrogen pressure and hydrogen to hydrocarbon ratio with low space velocities. Nevertheless, it is evident that our in-house synthesised catalysts are an order of magnitude more active than literature nickel

Table 5: Comparison between literature and in-house catalysts.

paper	**Dokjampa et al. 2007 [15]**	**Upare et al. 2013 [4]**	**Eliche-Quesada et al 2003 [31]**	**This study**
Catalyst	Ni/γ-Al_2O_3	Ni/SiO_2	Ni/Zr MSU	Ni/θ-Al_2O_3
Metal loading (%)	5	60	20	5
Catalyst form	Powder (20-40 mesh)	Powder (500 mesh)	Powder (16-20 mesh)	Pellets
Feed	tetralin	tetralin	5-20% tetralin in heptane	tetralin
Reactor	fixed bed	fixed bed	bench scale fixed bed	fixed bed
Reaction temperature (°C)	275	270	275	210
Reaction pressure (barg)	35.4	30	60	10
Reaction time	6h	1.8h	45min	30h
H_2/HC ratio	25	40	10.1	10.5
Space Velocity	WHSV = 1.5 h^{-1}	WHSV= 2.3 h^{-1}	LHSV=6 h^{-1}	WHSV = 5 h^{-1}
Conversion (%)	55	88.3	100	100
Trans-decalin (%)	75	75	72	52
Cis-decalin (%)	25	20	28	48
Rate (mol/g cat/h)	0.0028	0.00026	N/A	≥ 0.032

catalysts at much less forcing reaction conditions. It is also important to mention that our catalysts were evaluated as pellets hydrogenating solvent-free tetralin. Based on the experimental results of this work, the high activity of the in-house catalyst is more likely to be associated with the reaction conditions, which suggest that the literature catalysts would be more active if they were tested at lower temperature and pressure.

4. CONCLUSIONS

Tetralin hydrogenation was studied over a series of Ni/alumina catalysts prepared by different techniques using two precursors. The results revealed that tetralin hydrogenation over nickel catalysts was dependent upon the metal loading suggesting an absence of particle size effects for aromatic hydrogenation. However, catalyst deactivation and *trans*- to *cis*-decalin ratio was governed by the metal precursor with nickel carbonate catalysts showing a higher selectivity to *cis*-decalin and a lower rate of deactivation compared with the catalysts prepared from nickel nitrate. This change in selectivity was not related to tetralin conversion. The different behaviour can be explained by considering the mechanism of tetralin hydrogenation to decalin, which has aromatic hydrogenation as its first step to give octalins but olefin hydrogenation as the second step from octalins to decalins. The surface requirements for olefin hydrogenation are markedly different from that of aromatic hydrogenation and relate more to changes in the physical and textural properties of the synthesised catalyst (*i.e*. particle morphology). A similar pattern was observed with catalyst deactivation, in which, the catalysts prepared from nickel carbonate showed a much slower rate of deactivation even though they had slightly greater amount of deposited carbon. Suggesting no direct link between amount of carbon laydown and extent of deactivation. The TPO

of the deposited carbonaceous species was impacted by the preparation method with the absence of a low temperature combustion of molecular species when the catalysts were prepared by precipitation-deposition. Benchmarking the current catalyst system with the literature suggests that lower temperature and pressure may be more effective for tetralin hydrogenation

SUPPORTING INFORMATION

- Temperature Programmed Reduction (TGA-TPR) of fresh calcined support and meatal precursor
- Optimization of the Reaction Operating Conditions
- Reproducibility of the evaluation results
- Catalyst Post-Reaction Characterization

This information is available free of charge via the Internet at http://pubs.acs.org/.

ACKNOWLEDGMENT

Authors would like to acknowledge Saudi Aramco for supporting this research and would also like to thank Michael Beglan, Andrew Monaghan, and Drochaid research team for their contributions to this study.

AUTHOR INFORMATION

Corresponding Authors:-

S. David Jackson - Centre for Catalysis Research, School of Chemistry, University of Glasgow, Glasgow G12 8QQ, UK; orcid.org/0000-0003-1257-5533 Email: David.Jackson@glasgow.ac.uk

Ahmed K. AlAsseel – Research & Development Center, Saudi Aramco, Dhahran, Saudi Arabia. P.O.Box 6473, Dhahran 31311; Email: ahmed.asseel@aramco.com

AUTHOR CONTRIBUTIONS

Both authors contributed equally to the manuscript and have given approval to the final version.

REFERENCES

[1] Carrion, M. C.; Manzano, B. R.; Jalon, F. A.; Maireles-Torres, P.; Rodrıguez-Castellon, E.; Jimenez-Lopez, A. Hydrogenation of tetralin over mixed PtMo supported on zirconium doped mesoporous silica: Use of polynuclear organometallic precursors, *J. Molec. Catal. A: Chem*. **2006**, *252*, 31–39.

[2] Rautanen, P. A.; Lylykangas, M. S.; Aittamaa, J. R.; Krause, A. O. I. Liquid-phase hydrogenation of naphthalene and tetralin on Ni/Al_2O_3: kinetic modeling, *Ind. Eng. Chem. Res.* **2002**, *41(24)*, 5966–5975.

[3] Rautanen, P. A.; Aittamaa, J. R.; Krause, A. O. I.; Liquid phase hydrogenation of tetralin on Ni/Al_2O_3. *Chem. Eng. Sci.* **2001**, *56(4)*, 1247-1254.

[4] Upare, D. P.; Song, B. J.; Lee, C. W. Hydrogenation of tetralin over supported Ni and Ir catalysts, *Nanomaterials*, **2013**.

[5] Lin, S. D.; Song, C. Noble metal catalysts for low-temperature naphthalene hydrogenation in the presence of benzothiophene, *Catal. Today*. **1996**, *31(1-2)*, 93-104.

[6] Rase, H. F. Handbook of Commercial Catalysts: Heterogeneous Catalysts; CRC press: Texas, **2000**.

[7] Cooper, B. H.; Donnis, B. B.L. Aromatic saturation of distillates: an overview, *Appl. Catal. A.* **1996**, *137(2),* 203-223.

[8] Weitkamp, A. W. Deuteriation and deuterogenation of naphthalene and two octalins, *Catal.* **1966**, *6(3),* 431-457.

[9] Mason, R. T. Naphthalene, Kirk-Othmer Encyclopedia of Chemical Technology, **2000**, *17*

[10] Technical Resources, Inc. Tetralin and Decalin information, **1992**.

[11] Sapre, A. V.; Gates, B. C. Hydrogenation of aromatic hydrocarbons catalyzed by sulfided CoO-MoO_3/ γ-Al_2O_3: Reactivities and reaction networks, *Ind. and Eng. Chem. Proc. Design and Dev.* **1981**, *20(1),* 68–73.

[12] Huang, T.; Kang, B. Kinetic study of naphthalene hydrogenation over Pt/Al_2O_3 catalyst, *Ind. and Eng. Chem.* Res. **1995**, *34*, 1140-1148.

[13] Weitkamp A. W. Stereochemistry and mechanism of hydrogenation of naphthalenes on transition metal catalysts and conformational analysis of the products, *Adv. Catal*, **1968**, *18,* 1-110.

[14] Kirumakki, S. R.; Shpeizer, B. G.; Sagar, G. V.; Chary, K. V. R.; Clearfield, A. Hydrogenation of naphthalene over NiO/SiO_2–Al_2O_3 catalysts: Structure–activity correlation, *J. Catal.* **2006**, *242(2)*, 319-331.

[15] Dokjampa, S.; Rirksomboon, T.; Osuwan, S.; Jongpatiwut, S.; Resasco, D. E. Comparative study of the hydrogenation of tetralin on supported Ni, Pt, and Pd catalysts, *Catal. Today*. **2007**, *123(1-4),* 218-223.

[16] Haber J.; Block J. H.II; Delmon B. Manual of methods and procedures for catalyst characterization, *Pure & Appl. Chem.* **1995**, *67*, 1257-1306.

[17] Song S.; Sheng Z.; Liu Y.; Wang H.; Wu Z. Influences of pH value in deposition-precipitation synthesis process on Pt-doped TiO2 catalysts for photocatalytic oxidation of NO, *Envir. Sci.* **2012**, *24(8)* 1519–1524.

[18] Lok, C. M.; Gray, G.; Kelly, G. J. Catalysts with high cobalt surface area. US7501378, **2009**.

[19] Lok, C. M.; Verzijl, D.; Dijk, J. V.; Nickel catalyst on alumina support. US4490480A, **1983**.

[20] Vogelaar, B. M.; van Langeveld, A. D.; Kooyman, P. J.; Lok, C. M.; Bonne´, R. L. C.; Moulijn, J. A. Stability of metal nanoparticles formed during reduction of alumina supported nickel and cobalt catalysts *Catal. Today*, **2011**, *163*, 20–26.

[21] Gelder E. A. The hydrogenation of nitrobenzene over metal catalysts. PhD thesis, University of Glasgow, **2005**.

[22] Garba M. D. Valorisation of alkanes and alkynes by transhydrogenation in petrochemical processes, PhD thesis, University of Glasgow, 2017.

[23] Kim, P.; Kim, H.; Joo, J. B.; Kim, W.; Song, I. K.; Yi, J. Effect of nickel precursor on the catalytic performance of Ni/Al_2O_3 catalysts in the hydrodechlorination of 1,1,2-trichloroethane, *Mol. Catal. A: Chem.* **2006**, *256*, 178–183.

[24] Li, C.; Chen, Y. W.; Temperature-programmed-reduction studies of nickel oxide/alumina catalysts: effects of the preparation method, *Thermochimica Acta.* **1995**, *256*, 457 -465.

[25] Becerra, A. M.; Castro-Luna, A. E. An investigation on the presence of $NiAl_2O_4$ in a stable Ni on alumina catalyst for dry reforming. *Chil. Chem. Soc*. **2005**, *50*, 465-469.

[26] Chou, K. S.; Chang, S. C.; Huang, K. C. Study on the characteristics of nanosized nickel particles using sodium borohydride to promote conversion, *AZO Materials*. **2007**, *3*.

[27] Lai, W. C.; Song, C. Conformational isomerization of cis-decahydronaphthalene over zeolite catalysts, *Catal. Today*. **1996**, *31*, 171-181.

[28] Jongpatiwut, S.; Li, Z.; Resasco, D. E.; Alvarez, W. E.; Sughrue, E. L.; Dodwell, G. W. Competitive hydrogenation of poly-aromatic hydrocarbons on sulfur-resistant bimetallic Pt-Pd catalysts, *Appl. Catal. A: Gen*. **2004**, *262*, 241–253.

[29] Schmitz, A. D.; Bowers, G.; Song, C. Shape-selective hydrogenation of naphthalene over zeolite-supported Pt and Pd catalysts, *Catal. Today*. **1996**, *31(1-2)*, 45-56.

[30] Huang, Y.; Ma, Y.; Cheng, Y.; Wang, L.; Li, X. Supported nanometric platinum–nickel catalysts for solvent-free hydrogenation of tetralin, Catal. Commun. **2015**, *69*, 55-58.

[31] Eliche-Quesada, D.; Merida-Robles, J.; Maireles-Torres, P.; Rodrıguez-Castellon, E.; Jimenez-Lopez, A. Hydrogenation and ring opening of tetralin on supported nickel zirconium-doped mesoporous silica catalysts. Influence of the nickel precursor, *Langmuir*. **2003**, *19(12)*, 4985-4991.

[32] Doyle, A. M.; Shaikhutdinov, S. K.; Freund, H.-J. Surface-Bonded Precursor Determines Particle Size Effects for Alkene Hydrogenation on Palladium. *Angew. Chem. Int . Ed*. **2005**, *44*, 629 –631.

[33] Zaera, F. Regio-, Stereo-, and Enantioselectivity in Hydrocarbon Conversion on Metal Surfaces. *Acc. Chem. Res*., **2009**, *42*, 1152–1160.

[34] Argyle M. D.; Bartholomew C. H. Heterogeneous catalyst deactivation and regeneration: a review, Catalysts. **2015**, *5*, 145-269.

[35] Naccache C. Deactivation of acid catalysts, Deactivation and Poisoning of Catalysts. **1985**, 185–203.

[36] AlAsseel A. K. Tetralin hydrogenation over supported monometallic and bimetallic catalysts systems, PhD thesis, University of Glasgow, **2019.**

[37] Leguizamón Aparicio, M. S.; Ocsachoque, M. A.; Gazzoli, D.; Botto, I. L.; Lick, I. D. Total Oxidation of Naphthalene with Zirconia-Supported Cobalt, Copper and Nickel Catalysts. *Catalysts* **2017**, *7*, 293.

[38] Garcia, T.; Solsona, B.; Taylor, S. H. Naphthalene total oxidation over metal oxide catalysts. *Appl. Catal. B*, **2006**, *66*, 92–99

For Table of Contents (TOC)/Abstract graphic Only

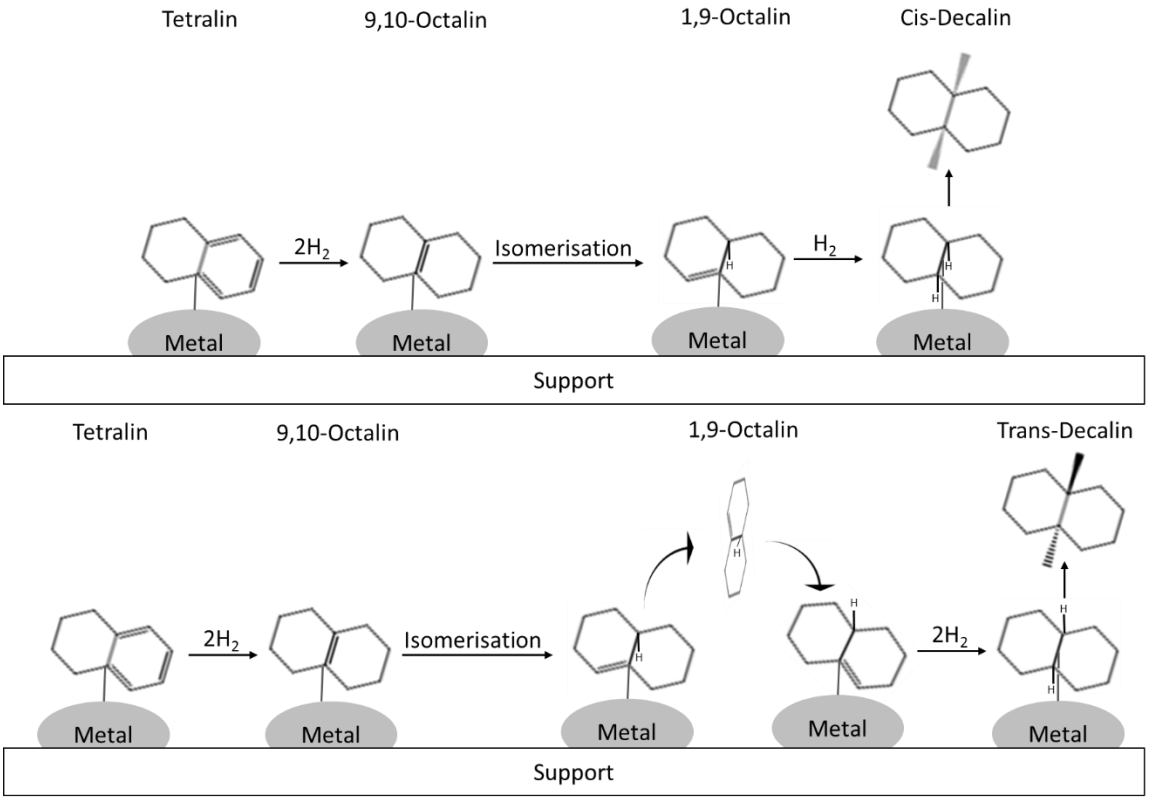

Illustration of cis-decalin (top) and trans-decalin (bottom) formation from tetralin through 9,10-octalin isomerisation.